Planetary and Space Science 57 (2009) 1950–1962

Contents lists available at ScienceDirect

Planetary and Space Science

journal homepage: www.elsevier.com/locate/pss

VIMS spectral mapping observations of Titan during the *Cassini* prime mission

Jason W. Barnes [a,*], Jason M. Soderblom [b], Robert H. Brown [b], Bonnie J. Buratti [c], Christophe Sotin [c], Kevin H. Baines [c], Roger N. Clark [d], Ralf Jaumann [e], Thomas B. McCord [f], Robert Nelson [c], Stéphane Le Mouélic [h], Sebastien Rodriguez [i], Caitlin Griffith [b], Paulo Penteado [b], Federico Tosi [j], Karly M. Pitman [c], Laurence Soderblom [k], Katrin Stephan [e], Paul Hayne [g], Graham Vixie [a], Jean-Pierre Bibring [l], Giancarlo Bellucci [j], Fabrizio Capaccioni [m], Priscilla Cerroni [m], Angioletta Coradini [j], Dale P. Cruikshank [n], Pierre Drossart [o], Vittorio Formisano [j], Yves Langevin [l], Dennis L. Matson [c], Phillip D. Nicholson [p], Bruno Sicardy [o]

[a] *Department of Physics, University of Idaho, Engineering-Physics Building, Moscow, ID 83844, USA*
[b] *Department of Planetary Sciences, University of Arizona, Tucson, AZ 85721, USA*
[c] *Jet Propulsion Laboratory, California Institute of Technology, 4800 Oak Grove Drive, Pasadena, CA 91109, USA*
[d] *United States Geological Survey, Denver, CO 80225, USA*
[e] *DLR, Institute of Planetary Research, Rutherfordstrasse 2, D-12489 Berlin, Germany*
[f] *The Bear Fight Center, P.O. Box 667, 22 Fiddler's Road, Winthrop, WA 98862, USA*
[g] *Earth and Space Sciences Dept. University of California, Los Angeles 595 Charles Young Drive East Los Angeles, CA 90095, USA*
[h] *Laboratoire de Planétologie et Géodynamique, CNRS UMR6112, Université de Nantes, France*
[i] *Laboratoire AIM, Centre d'ètude de Saclay, DAPNIA/Sap, Centre de l'Orme des Merisiers, bât. 709, 91191 Gif/Yvette Cedex, France*
[j] *Instituto di Fisica dello Spazio Interplanetario, Consiglio Nazionale delle Richerche, Rome 00133, Italy*
[k] *U.S. Geological Survey, Astrogeology Team, 2255 N. Gemini Dr., Flagstaff, AZ 86001, USA*
[l] *Institut d'Astrophysique Spatiale, Université de Paris-Sud, Orsay 91405, France*
[m] *Istituto di Astrofisica Spaziale e Fisica Cosmica, Consiglio Nazionale delle Richerche, Rome 00133, Italy*
[n] *NASA Ames Research Center, Moffett Field, CA 94035, USA*
[o] *Observatoire de Paris, Meudon, France*
[p] *Department of Astronomy, Cornell University, Ithaca, NY 14853, USA*

ARTICLE INFO

Article history:
Received 5 December 2008
Received in revised form
31 March 2009
Accepted 21 April 2009
Available online 5 May 2009

Keywords:
Titan
Cassini
VIMS

ABSTRACT

This is a data paper designed to facilitate the use of and comparisons to *Cassini*/visual and infrared mapping spectrometer (VIMS) spectral mapping data of Saturn's moon Titan. We present thumbnail orthographic projections of flyby mosaics from each Titan encounter during the *Cassini* prime mission, 2004 July 1 through 2008 June 30. For each flyby we also describe the encounter geometry, and we discuss the studies that have previously been published using the VIMS dataset. The resulting compliation of metadata provides a complementary big-picture overview of the VIMS data in the public archive, and should be a useful reference for future Titan studies.

1. Introduction

Though it was not initially designed for imaging Titan's surface, *Cassini*'s Visual and Infrared Mapping Spectrometer (VIMS) has proven flexible enough to have made fundamental contributions there. On Titan's surface, VIMS has seen a possible cryovolcano (Sotin et al., 2005), discovered and mapped new spectral terrain types (Barnes et al., 2005), and directly detected the presence of ethane in the south polar lake Ontario Lacus (Brown et al., 2008). In Titan's atmosphere VIMS has watched the vertical evolution of convective clouds (Griffith et al., 2005), discovered a polar ethane cloud (Griffith et al., 2006), and measured the atmospheric abundance of carbon monoxide (Baines et al., 2006).

The *Cassini*/VIMS dataset for Titan is available at the NASA Planetary Data System (PDS): http://pds.nasa.gov/. The headers for individual data cubes include metadata that describe them, including exposure time, cube dimensions, and other characteristics. We will not describe those details here. The PDS data do not, however, include a big-picture overview of the dataset as a whole. We attempt to provide that overview here. We describe here only those Titan data obtained in spectral mapping mode, and do not include solar and stellar occultations in the present work.

* Corresponding author.
E-mail address: jwbarnes@uidaho.edu (J.W. Barnes).

0032-0633/$ - see front matter © 2009 Elsevier Ltd. All rights reserved.
doi:10.1016/j.pss.2009.04.013

In this data paper, we display and describe the VIMS spectral mapping data for each of the Titan flybys during the *Cassini*'s four-year primary mission between 2004 July 1 and 2008 June 30, placing each into context with the rest of the dataset and with previously published work. The purposes of this paper are (1) to serve as a roadmap for VIMS data for those intending to use it for scientific purposes and (2) to allow for easy intercomparison between the VIMS dataset and complementary datasets such as those from the *Cassini* Imaging Science Subsystem (ISS) and RADAR and Earth-based telescopic observations.

2. Dataset

VIMS acquires spectral mapping cubes up to 64 × 64 pixels in *X* (samples) and *Y* (lines), with 352 wavelength channels from two subinstruments, 96 wavelengths from the visual channel from 0.3−1 μm and 256 wavelengths in the infrared channel from 0.88−5.2 μm (Brown et al., 2004). There are several spectral "windows" in the near-infrared where Titan's atmospheric gases are transmissive, despite its hazes' scattering, and therefore where observations of the surface are possible. These include (but are not limited to) 0.76, 0.83, 0.94, 1.08, 1.28, 1.6, 2.0, 2.8, and 5 μm.

The *Cassini* Imaging Science Subsystem (ISS) camera uses the 0.94 μm window that is strongly affected by atmospheric haze scattering. The 0.94, 1.08, and 1.28 μm windows show enhanced reflectivity relative to the longer wavelength windows for water ice. The 2.0 μm window represents VIMS' best window for surface imaging, with a compromise between atmospheric scattering and reflected flux from Titan's surface (Jaumann et al., 2006). The wings of the 2.0 μm window have been used as an altitude discriminant (Griffith et al., 2005), but the wings of other windows could be used similarly. The 2.8 μm window shows an as-yet-unexplained double-peaked structure that may be diagnostic of H_2O and/or CO_2 ice. The 5 μm channel shows the least atmospheric interference, shows the greatest surface reflectance contrast relative to the other windows, and is also the widest allowing for robust detection of absorption features. As the most useful of these windows are those at longer wavelengths, the data that we present specifically here are those from the infrared channel.

For global orientation and identification of individually named features that we refer to below, we present a global cylindrical map of Titan as seen from VIMS in Fig. 1. The map incorporates data from the Ta, T4, T8, T9, T11, T13, T28, T32, T33, and T34 Titan flybys, and so is not yet complete.

The colors used in the map and in the left-hand individual flyby orthographic projections below are 5 μm as red, 2.0 μm as green, and 1.28 μm as blue. These colors are all within the atmospheric windows, and so all predominantly represent surface contributions to the measured *I*/*F*. They were chosen because 2.0 μm represents the best compromise between surface contribution signal-to-noise ratio and low atmospheric scattering, 5 μm has the strongest spectral changes across Titan when compared to other wavelengths, and 1.28 μm represents areas that are possibly rich in water–ice. This color scheme is described further in Barnes et al. (2007).

The color scheme used for the right-hand maps in the flyby thumbnails brings out atmospheric features. This cloud-color scheme was designed for Griffith et al. (2005) with the intent to make images intuitive by having surface features colored in green, haze in red, and clouds in blue/white. The scheme neatly delineates the oft-confused (by some casual observers) clouds and haze from one another. In achieving this delineation, the resulting color scheme is a bit unconventional with red mapped to the shortward edge of the 2-μm window at 1.969 μm, green in the 2.7-μm window at 2.696 μm, and blue off the shortward end of the 2.7-μm window at 2.647 μm.

The combination of the left-hand surface images with the right-hand atmosphere images makes it possible to quickly identify which features are due to surface reflection and which are located above the surface for any given flyby.

3. Flyby descriptions

We present global orthographic projections from flybys Ta through T44 in Figs. 2–6. We first mosaic individual cubes together into a cylindrical map with resolution appropriate

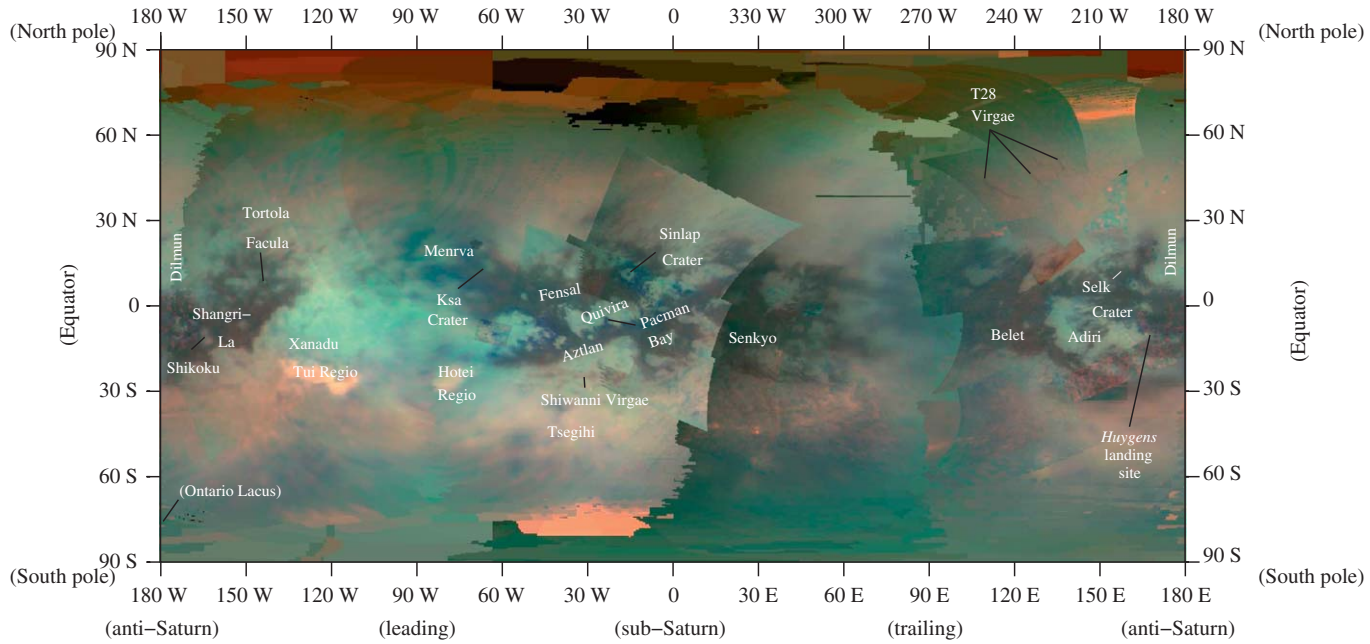

Fig. 1. Global VIMS cylindrical map of Titan with RED = 5 μm, GREEN = 2.0 μm, and BLUE = 1.28 μm.

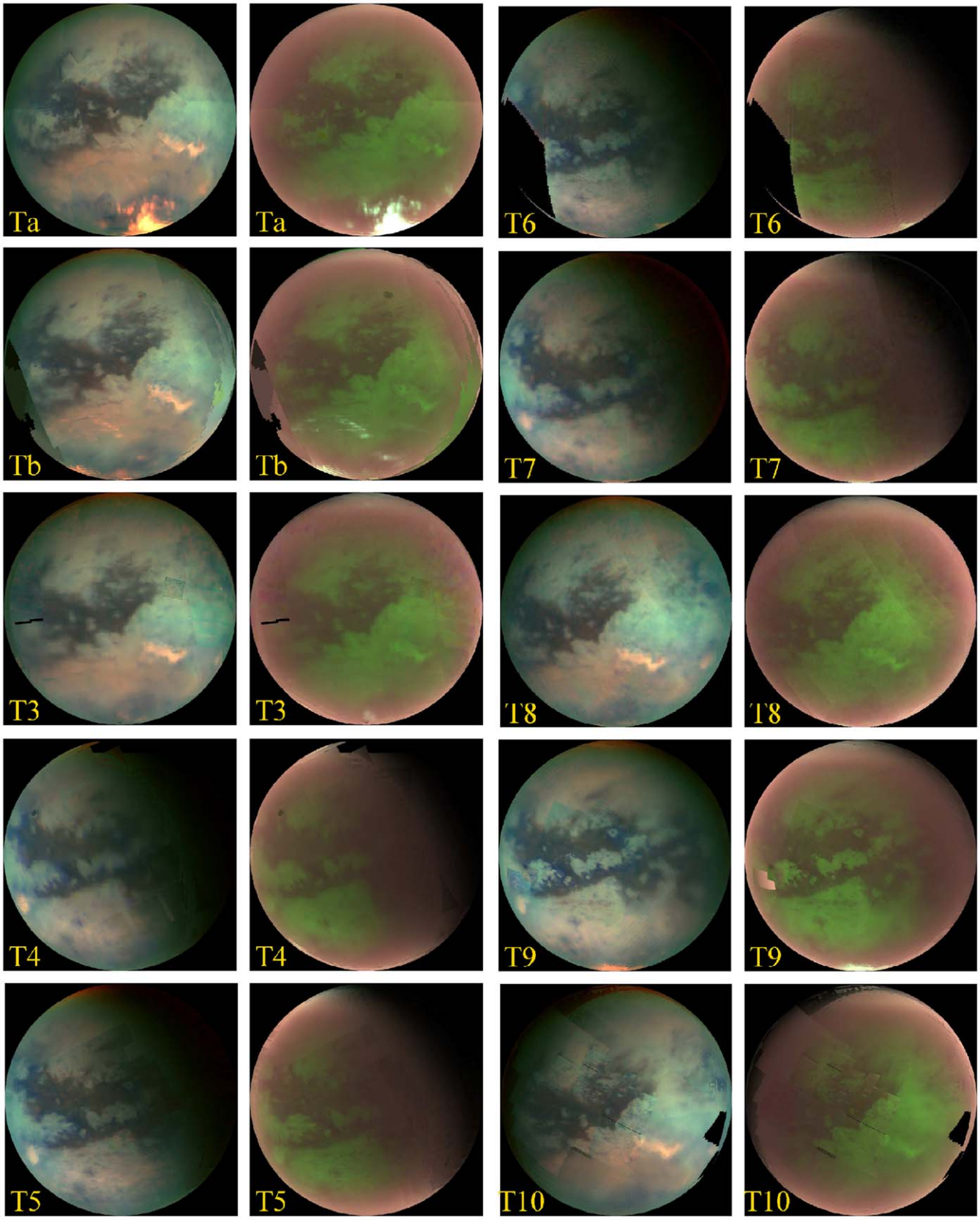

Fig. 2. Orthographic projections of flybys Ta through T5 (left) and T6 through T10 (right); see text.

for the data, and then convert the cylindrical map into an orthographic projection from above the sub-spacecraft point with north up.

The dates, sub-spacecraft latitude and longitude on both ingress and egress, and subsolar latitude and longitude, along with the average phase angle (Sun–Titan-spacecraft), are shown in

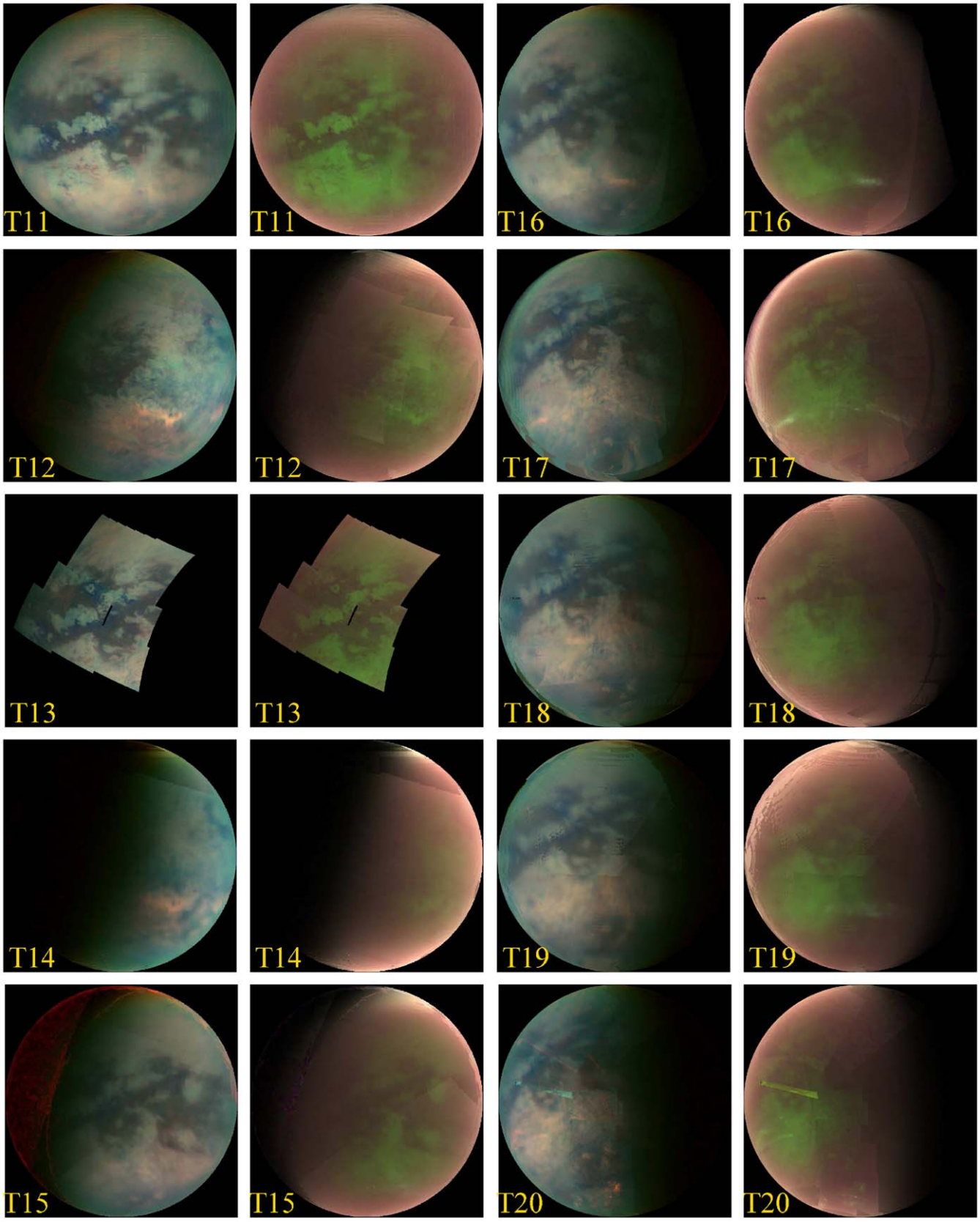

Fig. 3. Orthographic projections of flybys T11 through T15 (left) and T16 through T20 (right); see text.

Table 1. The subsolar location indicated in the tables is that for the spacecraft's closest approach to Titan. The phase angles on ingress and egress were both calculated using this average subsolar point. As each Titan encounter lasts a total of ~2 days, the phase angle for any given cube may vary from the indicated value by up to 20°.

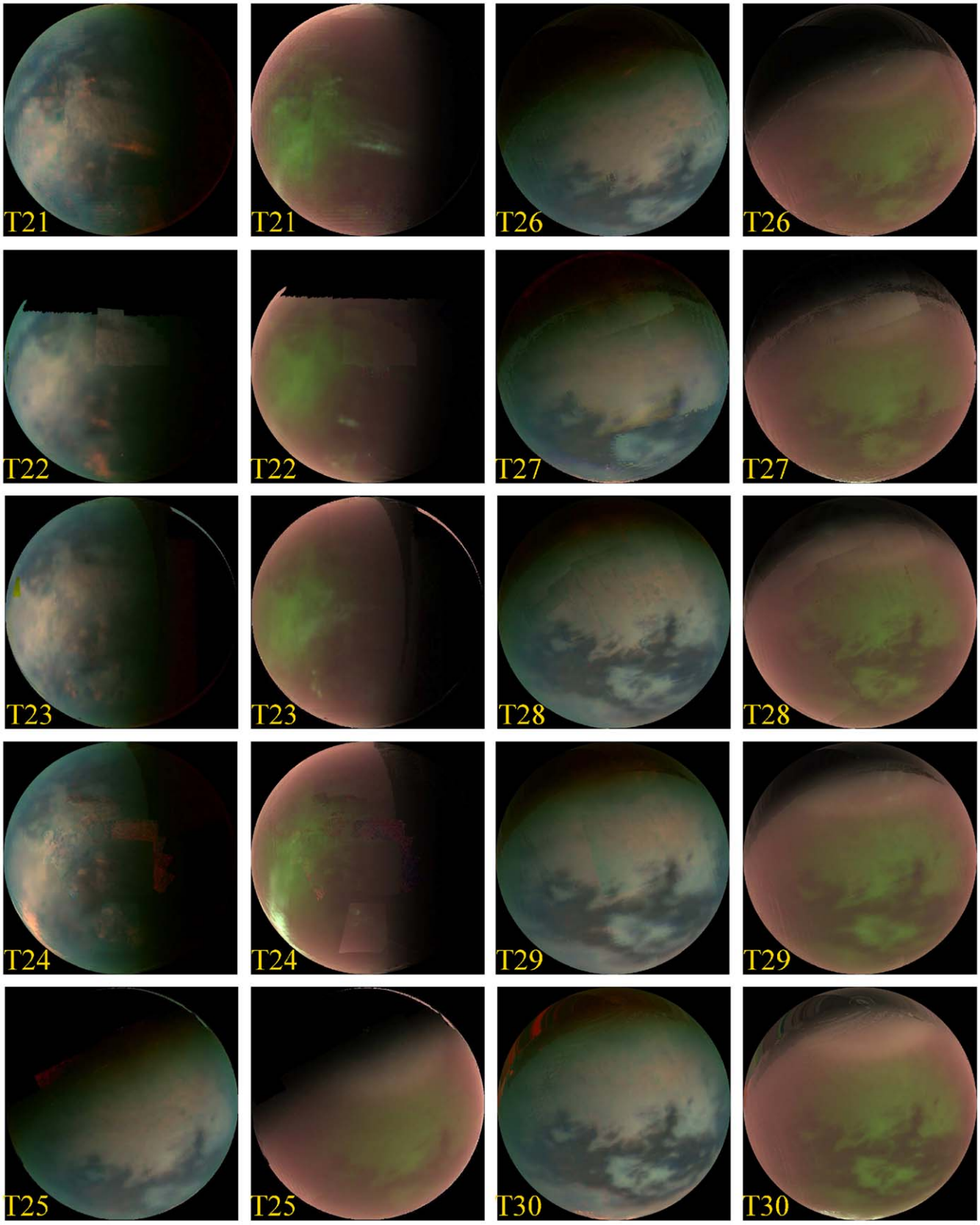

Fig. 4. Orthographic projections of flybys T21 through T25 (left) and T26 through T30 (right); see text.

For each of the Titan close encounters Ta through T44 (Table 1) show the asymptotic sub-spacecraft points for ingress and egress. We do not show the closest-approach latitude and longitude because those values are nearly irrelevant for VIMS. VIMS observed at closest approach for only four flybys: T20, T24, T35, and T38. The remaining closest approaches were allocated

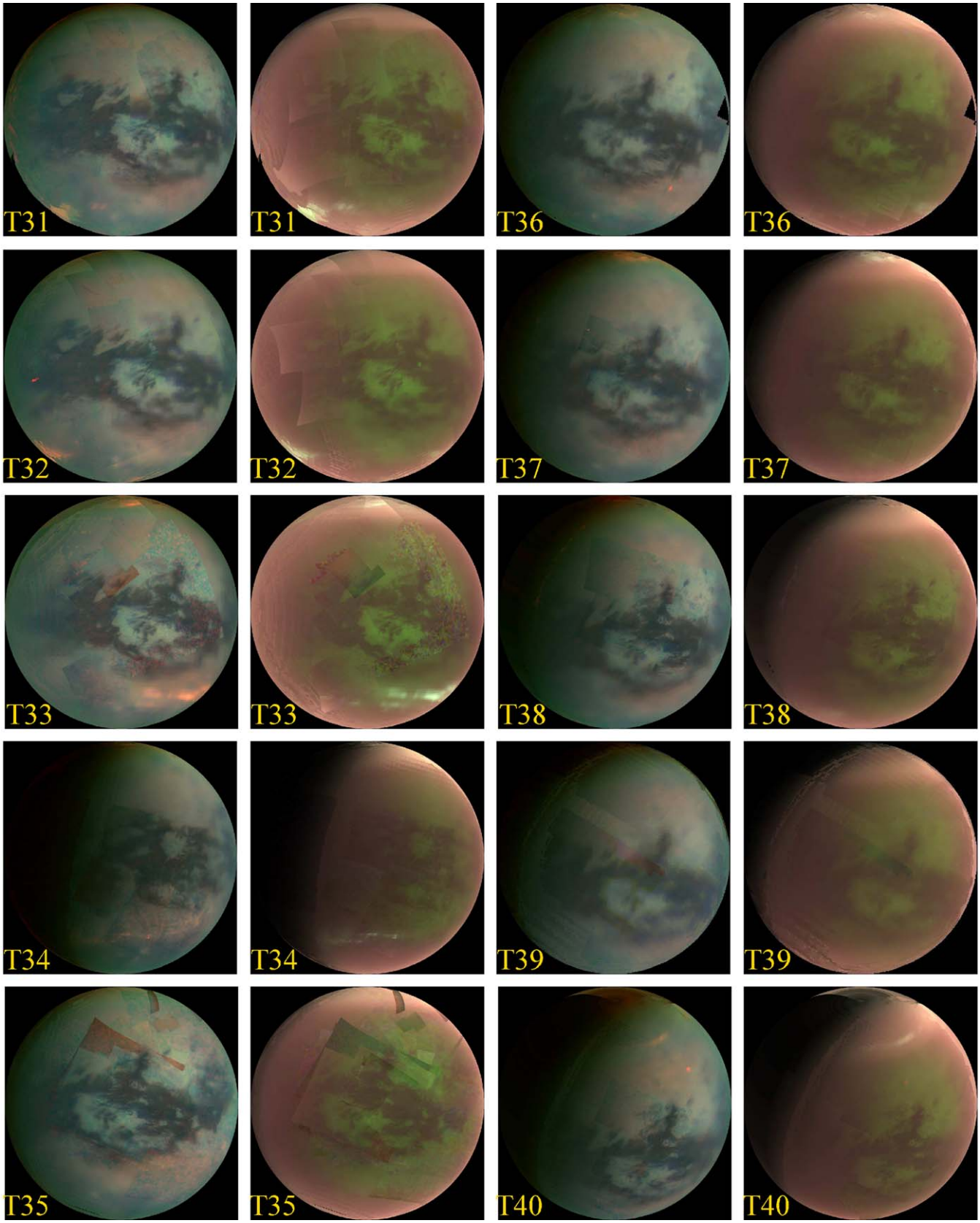

Fig. 5. Orthographic projections of flybys T31 through T35 (left) and T36 through T40 (right); see text.

to other *Cassini* instruments. Therefore VIMS data are acquired while *Cassini* is on approach to Titan and while it is receding from Titan. The subspacecraft ingress and egress locations in Table 1 represent values derived from SPICE kernels (Acton, 1999) for an existing VIMS cube acquired while ~200,000 km from Titan on that flyby. These values are broadly representative

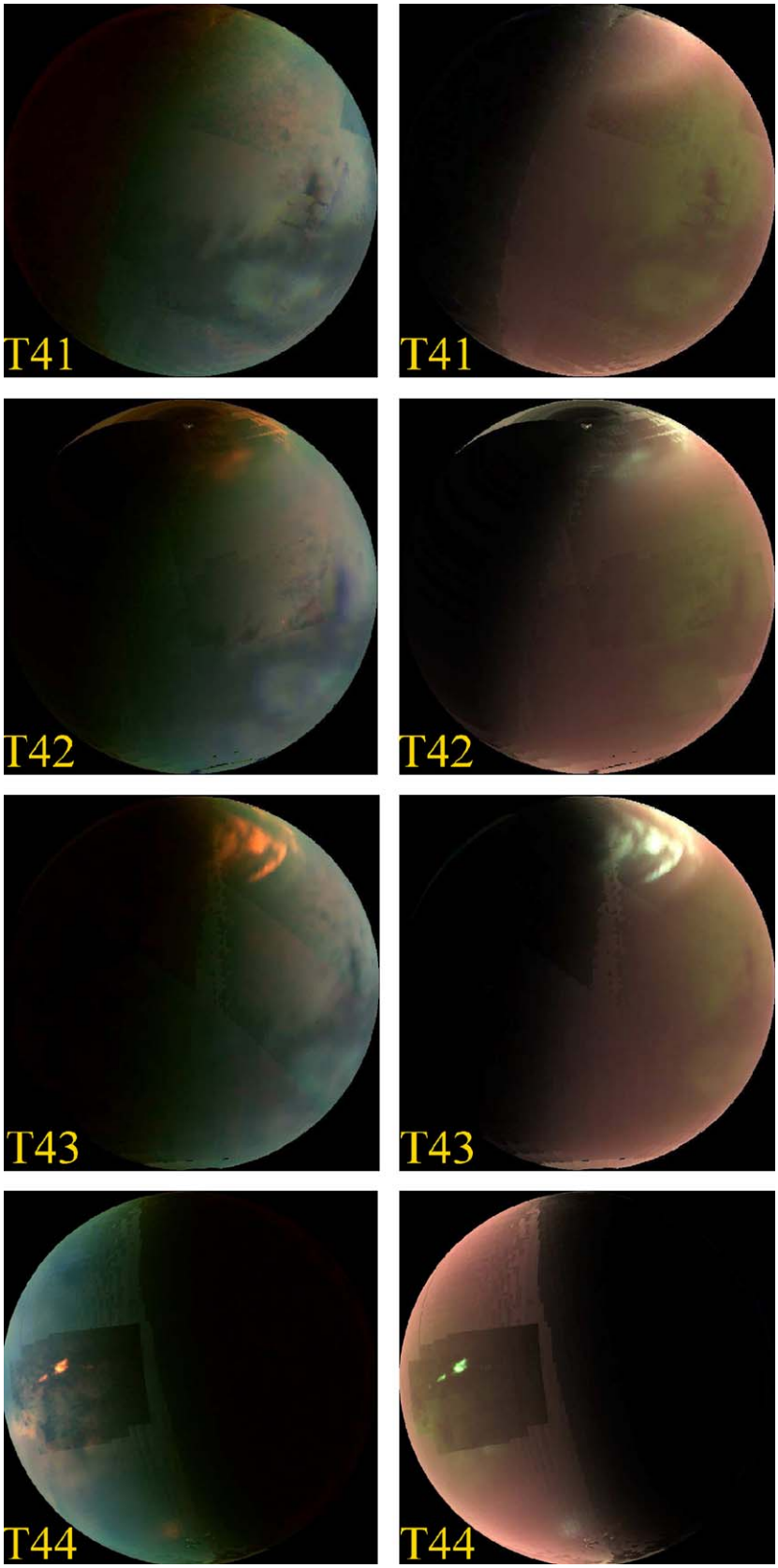

Fig. 6. Orthographic projections of flybys T41 through T44; see text.

Table 1
VIMS prime mission Titan flyby observations.

Flyby	Date	Subsolar point	Ingress sub-S/C point and phase	Egress sub-S/C point and phase	Best spatial sampling (km)
T0	2004 July 2	24.1°S 59°W	63°S 22°E $\phi = 65°$	N/A	85
Ta	2004 October 26	23.2°S 165°W	15°**S** 161°**W** $\phi = 9°$	11°N 8°E $\phi = 166°$	2.6
Tb	2004 December 13	22.8°S 147°W	9°**S** 154°**W** $\phi = 15°$	4°N 9°E $\phi = 150°$	1.35
T3	2005 February 15	22.2°S 155°W	3°**S** 151°**W** $\phi = 20°$	0°N 14°E$\phi = 155°$	7
T4	2005 March 31	21.8°S 79°W	1°**N** 17°**W** $\phi = 65°$	2°S 143°E $\phi = 133°$	1.2
T5	2005 April 16	21.6°S 79°W	4°**N** 19°**W** $\phi = 64°$	(no VIMS)	5
Rev9	2005 June 6	21.1°S 145°W	75°S $\phi = 71°$	50°W C/A	109
T6	2005 August 22	20.3°S 75°W	10°**N** 20°**W** $\phi = 62°$	10°S 143°E $\phi = 132°$	31
T7	2005 September 7	20.1°S 74°W	7°**N** 20°**W** $\phi = 60°$	(no VIMS)	52
T8	2005 October 28	19.6°S 139°W	0°**S** 146°**W** $\phi = 21°$	0°N 15°E $\phi = 148°$	42
T9	2005 December 26	18.9°S 45°W	0°**S** 15°**W** $\phi = 35°$	0°N 155°E $\phi = 153°$	2.9
T10	2006 January 15	18.7°S 127°W	0°**S** 148°**W** $\phi = 28°$	0°N 11°E $\phi = 135°$	3.9
T11	2006 February 27	18.1°S 17°W	0°**S** 5°**W** $\phi = 28°$	0°N 153°E $\phi = 135°$	18
T12	2006 March 18	17.9°S 96°W	0°**S** 147°**W** $\phi = 53°$	0°S 13°E $\phi = 109°$	7
T13	2006 April 30	17.3°S 13°E	0°**S** 15°**W** $\phi = 33°$	(no VIMS)	10
T14	2006 May 20	17.1°S 66°W	0°**S** 149°**W** $\phi = 83°$	0°**S** 4°**E** $\phi = 71°$	48
T15	2006 July 2	16.5°S 42°E	0°**S** 0°**W** $\phi = 45°$	0°N 154°E $\phi = 111°$	55
T16	2006 July 22	16.3°S 36°W	1°N 147°W$\phi = 110°$	8°**S** 17°**E** $\phi = 52°$	30
T17	2006 September 7	15.6°S 34°W	9°N 145°W $\phi = 113°$	12°**S** 22°**E** $\phi = 54°$	7.5
T18	2006 September 23	15.4°S 34°W	13°N 138°W $\phi = 107°$	20°**S** 25°**E** $\phi = 56°$	1.5
T19	2006 October 9	15.2°S 33°W	22°N 136°W $\phi = 107°$	28°**S** 27°**E** $\phi = 57°$	40
T20	2006 October 25	15.0°S 32°W	29°N 132°W $\phi = 106°$	30°**S** 36°**E** $\phi = 64°$	0.49
T21	2006 December 12	14.3°S 30°W	31°N 124°W $\phi = 101°$	36°**S** 34°**E** $\phi = 61°$	20
T22	2006 December 28	14.1°S 29°W	38°N 127°W $\phi = 105°$	43°**S** 35°**E** $\phi = 62°$	7.4
T23	2007 January 13	13.9°S 29°W	45°N 119°W $\phi = 100°$	50°**S** 42°**E** $\phi = 67°$	25
T24	2007 January 29	13.7°S 28°W	53°N 115°W $\phi = 99°$	55°**S** 50°**E** $\phi = 72°$	1.7
T25	2007 February 22	13.4°S 153°E	(no VIMS)	51°**N** 121°**E** $\phi = 70°$	54
T26	2007 March 10	13.1°S 153°E	49°S 37°W $\phi = 117°$	45°**N** 125°**E** $\phi = 63°$	25
T27	2007 March 26	12.9°S 154°E	43°S 31°W $\phi = 124°$	38°**N** 133°**E** $\phi = 55°$	24
T28	2007 April 10	12.7°S 155°E	36°S 27°W $\phi = 131°$	31°**N** 137°**E** $\phi = 47°$	11
T29	2007 April 26	12.5°S 155°E	29°S 25°W $\phi = 138°$	23°**N** 137°**E** $\phi = 40°$	53
T30	2007 May 12	12.2°S 156°E	21°S 21°W $\phi = 147°$	16°**N** 143°**E** $\phi = 31°$	48
T31	2007 May 28	12.0°S 156°E	13°S 22°W $\phi = 155°$	10°**N** 153°**E** $\phi = 22°$	11
T32	2007 June 13	11.8°S 157°E	8°S 19°W $\phi = 160°$	2°**N** 142°**E** $\phi = 20°$	12
T33	2007 June 29	11.5°S157°E	1°S 17°W $\phi = 166°$	0°**N** 148°**E** $\phi = 15°$	12
T34	2007 July 19	11.3°S 78°E	0°N 143°W $\phi = 138°$	6°**S** 40°**E** $\phi = 38°$	8
T35	2007 August 31	10.6°S 173°W	1°N 8°W $\phi = 162°$	2°**S** 155°**E** $\phi = 33°$	10
T36	2007 October 2	10.2°S 172°W	(no VIMS)	2°**N** 150°**E** $\phi = 40°$	25
T37	2007 November 19	9.5°S 171°W	3°S 14°W $\phi = 154°$	5°**N** 144°**E** $\phi = 47°$	0.69
T38	2007 December 5	9.2°S 171°W	7°S 21°W $\phi = 146°$	12°**N** 138°**E** $\phi = 55°$	0.33
T39	2007 December 20	9.0°S 170°W	17°N 21°W $\phi = 149°$	19°**N** 139°**E** $\phi = 58°$	58
T40	2008 January 8	8.7°S 170°W	20°S 25°W $\phi = 135°$	22°**N** 131°**E** $\phi = 65°$	1.95
T41	2008 February 22	8.0°S 168°W	23°S 31°W $\phi = 128°$	26°**N**123°**E** $\phi = 75°$	26
T42	2008 March 25	7.5°S 167°W	27°S 38°W $\phi = 120°$	30.5°**N** 115°**E** $\phi = 84°$	10
S40	2008 April 26	7.1°S 169°W	69°N $\phi = 92°$	92°W (C/A)	190
T43	2008 May 12	6.8°S 165°W	30°S 44°W $\phi = 113°$	29°**N** 107°**E** $\phi = 92°$	81
T44	2008 May 28	6.6°S 164°W	28°S 47°W $\phi = 110°$	27°**N** 100°**E** $\phi = 98°$	11

of all of the cubes from each flyby for ingress and egress, respectively.

Due to the flyby nature of the Titan encounters, in general either the ingress or the egress observations were acquired over the day side. We depict this in Table 1 by indicating the encounter leg with the lowest phase angle in boldfaced font.

The specified best spatial sampling is the value for the finest spatial sampling of a single pixel during the encounter. Hence the value is not intended to be broadly representative of a given flyby. T4 for instance has a good best spatial sampling of 1.2 km/pixel, but only two cubes were acquired with anything near that sampling. The remainder of the T4 data are of global scope with spatial sampling greater than 60 km/pixel. In contrast, on Tb a wide range of cubes exist with spatial samplings between that indicated (1.35 km) and one pixel per degree (45 km/pixel).

We show a selected set of fully mosaiced orthographic projections for encounter legs with high phase angles (i.e., over Titan's nightside) in Fig. 7. These data exist for most close flybys, but at lower spatial resolution than for dayside data.

We also show in Fig. 7 single data cube images (not orthographic projections) from three non-targeted Titan flybys. These flybys have closest approaches greater than 300,000 km from Titan. They were obtained because they provide unusual observation geometries that complement the close flyby data. Given VIMS limited inherent angular sampling (0.5 mrad/pixel), the spatial sampling of these long-distance data is very coarse (see Table 1).

3.1. Saturn orbit insertion encounter (T0)

The first VIMS spectral mapping of Titan occurred just after Saturn orbit insertion on the non-targeted T0 flyby (Fig. 7). In order to conserve data volume, the observations from this flyby are "spectrally edited", meaning that not all VIMS spectral channels were downlinked, only those that were thought to be interesting at the time that the observations were planned. The resulting dataset is difficult to work with

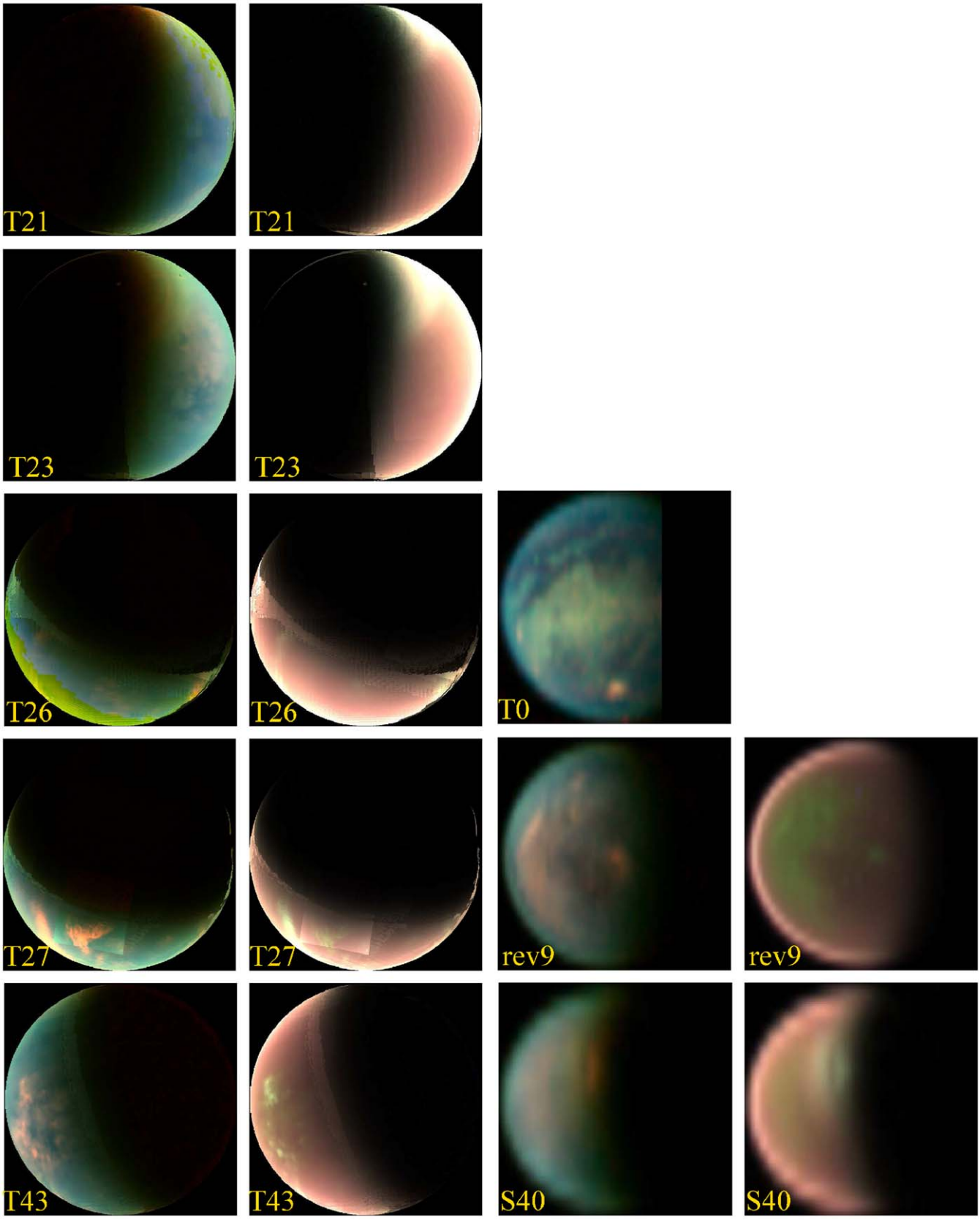

Fig. 7. Selected orthographic projections from Titan's nightside (left), and from non-targeted far-flybys of Titan (right); see text.

and to compare to other flyby datasets. We do not show a cloud-color image from T0 in Fig. 7 because the unusual spectral channels used in the cloud-color scheme were edited out of the data that were returned to Earth. Spectral editing was deemed to be not worth its costs, and the mode has not been used since.

Because they were the first data acquired, the observations from this flyby led to important discoveries studied in depth by several authors despite the flyby's coarse spatial resolution. Baines et al. (2005) showed clouds, 3.3 μm methane fluorescence, and spectra, while Brown et al. (2006) described the view of Titan's surface as well as T0's atmospheric features. Adriani et al. (2005) used these data to derive estimates of Titan's 2-μm surface albedo using RADTRAN radiative transfer models. Baines et al. (2006) discovered nighttime carbon monoxide emission from the T0 data that they used to infer ongoing geological activity.

3.2. Low-phase-angle encounters (Ta, Tb, T3)

The first three close Titan encounters with VIMS observations, Ta, Tb, and T3, were designed for low-phase optical remote sensing observations (see Fig. 2). No VIMS data were acquired on the Tc pass because it was devoted to relaying communications from the *Huygens* probe.

Ta was the first close Titan flyby made by *Cassini*. As such it was used by several initial global surveys. McCord et al. (2006) analyzed the Ta data to place initial constraints on surface composition. Buratti et al. (2006) inferred a dichotomy in the surface phase function that they interpreted to imply greater topographic roughness in bright terrains relative to dark ones. This interpretation has been bourne out by subsequent RADAR observations. Nelson et al. (2006) used the Ta data as part of a larger photometric study that incorporated data from other flybys (T0, Tb, T3, T4, and T5) as well.

In addition to global approach coverage, on the Ta flyby VIMS acquired a range of moderate and fine-resolution spectral mapping cubes. An ISS ridealong sequence mapped by Jaumann et al. (2006) has scattered, small VIMS cubes (12×12) as driven by the short pointing dwell times that were used early in the mission before Titan's observational characteristics were well understood. A high priority for this flyby was the observations of the Huygens landing site that were analyzed by Rodriguez et al. (2006) and Soderblom et al. (2007) in terms of surface composition and properties, and that were used by Baines et al. (2005) to illustrate clouds and atmospheric scattering effects on surface visibility. Serendipitous targeting for the fine-resolution cubes allowed the discovery of a charismatic surface feature, "the Snail" (officially Tortola Facula), that Sotin et al. (2005) interpreted as a cryovolcanic edifice.

Both the snail cubes and the landing site cubes were taken while *Cassini* was too deep in Titan's atmosphere to maintain pointing using its reaction wheels. The spacecraft's alternate pointing system, the thrusters, are decidedly less precise, and so the pointing during these cubes is highly erratic. When cylindrically mapping these cubes for Fig. 2 we used nearest-neighbor interpolation instead of the usual Lanczos interpolation because nearest-neighbor provides more robust images under these irregular geometries. After the in-atmosphere performance characteristics of the spacecraft as measured on the Ta flyby, subsequent prime mission flybys' periapses were raised far enough out of the atmosphere such that thruster-pointing has not been necessary on any subsequent flybys.

The Tb ingress observations cover a similar area to those from Ta under nearly identical illumination conditions. They were incorporated into the global investigations of Nelson et al. (2006) and (McCord et al., 2008a) and into the Jaumann et al. (2006) mosaics as well. Griffith et al. (2005) used time-lapse global spectral mapping to chart the vertical evolution of some of Titan's mid-latitude convective clouds; the clouds themselves were shown in Baines et al. (2005) as well. Looking up to the high emission-angle views of the north pole on Tb (as well as T6 and T7), Griffith et al. (2006) identified a polar ethane cloud. The moderate- and fine-resolution cubes from Tb were designed to complement those from Ta in terms of surface coverage. Barnes et al. (2006) used moderate-resolution Tb views of western Tui Regio to identify possible flow features there, in concert with ISS imaging. Rodriguez et al. (2006) used Tb data in their *Huygens* landing site analysis, and Barnes et al. (2007) identified a wide, sinuous channel within Xanadu that correlates with channels seen by RADAR there on T13.

The T3 observations have geometry and illumination conditions very similar to Ta and Tb, but at much coarser spatial resolution and with sparse coverage. A few quality cubes cover modest areas with one east of Tortola Facula and another in northwestern Xanadu.

3.3. Fensal–Aztlan flybys (T4–T7, T9, T11, T13, T15)

The orbital dynamics of mission design led the flybys up through T15 to have their approach asymptotes over the same two regions. The Fensal–Aztlan (the "H") flybys, T4–T7, T9, T11, T13, and T15, have subspacecraft longitudes between 0°W and 20°W on ingress, a geometry in which views of Fensal–Aztlan figure prominently. The spacecraft orbital inclination around Saturn was near 0° for these flybys, and so these flybys' subspacecraft points all lie on Titan's equator.

T4 featured coarse-resolution global coverage and a pair of fine-resolution cubes centered east of Menrva Crater and north of Ksa Crater in northwestern Fensal. The fine-resolution cubes allowed Barnes et al. (2007) to first identify the longitudinal sand dunes seen by RADAR (Lorenz et al., 2006) in the VIMS dataset. These data were further analyzed by Barnes et al. (2008), who used them to measure the dune orientations and topography, and by LeCorre et al. (2008) who used them in concert with the T20 closest-approach noodle to study possible cryolava flows.

On T5 VIMS acquired an excellent moderate-resolution mosaic of Fensal–Aztlan, shown by Jaumann et al. (2006), that extends from just east of Ksa Crater in the west and over to Titan's terminator east of Sinlap Crater on the eastern side. Le Mouélic et al. (2008) used this, our best view of Sinlap Crater, to map the spectral units in its environs and to identify a possible central peak within the 80-km-diameter crater. This mosaic also provided context for the later T20 closest-approach noodle that transected the western portion of the T5 moderate-resolution data (Barnes et al., 2008). Barnes et al. (2005) noted the unusual, 5-μm-bright spectrum of Hotei Regio from the T5 near-global views. Nelson et al. (2009) used the T4 and T5 (along with T0, T6–T10, and T12) Hotei Regio views in their long-term monitoring of the photometric stability of Hotei Regio.

Because they have complementary surface coverage to the earlier Ta and Tb flybys, the T4 and T5 flybys were used by Buratti et al. (2006) to broaden the surface coverage of their surface phase function measurements.

T6 and T7 have only coarse-resolution VIMS data, but their more northerly sub-solar latitude allowed Griffith et al. (2006) to use them to discover the north polar ethane cloud, which has become more visible as Titan has since moved toward northern spring and the terminator has shifted northward.

Some of VIMS' best regional coverage occurred on the T9 flyby. This flyby had an unusually high closest-approach altitude of 10411 km from Titan's surface; typical closest approaches were between 950 and 3000 km. The high altitude meant that VIMS could acquire long integration observations over large areas at moderate spatial resolution. As such the T9 flyby has proven valuable for global-scale spectral studies. Barnes et al. (2007) used this for their global maps and spectral unit identification, finding

that spectral character changes strongly as a function of latitude. Soderblom et al. (2007) used the T9 dataset, particularly the cubes of Quivira and environs, to identify three spectral endmembers, a linear combination of which can model the surface reflectivity for most of Titan's tropics. Both McCord et al. (2008b) and Clark et al. (2007) used the T9 data to search for spectral absorption features within the 5-μm window, finding a 4.92 μm absorption feature and benzene, respectively.

While following the surface during and past closest approach and into high phase angle viewing geometries on T9, VIMS acquired moderate-fine-resolution spectral mapping of the area east of Xanadu that Barnes et al. (2007) used to track channels and measure their width, and to compare VIMS spectra with synthetic aperture RADAR imaging. The strangely shaped pink area on the left of the T9 cloud-color image shown in Fig. 2 is one of the high-phase-angle lookback cubes, accounting for the greater influence of haze in that image.

On the T11 flyby VIMS imaged Quivira and the Shiwanni Virgae. Due to an oversight when the sequence design was updated, these data show severe smear when VIMS was continuing to observe while the spacecraft turned to its new target. Because VIMS only observes with one pixel at a time, however, for the images shown in Fig. 3 we used the SPICE kernels to reconstruct the pointing for each pixel independently in order to recover the images.

T13 has just two moderate-resolution mosaics, a 2×3 of eastern Fensal–Aztlan and a 1×6 of the area northeast of there in hi-res mode. Due to a downlink error most of the VIMS data from this flyby were not received, including the lower resolution context from this flyby. The data that were received provide one of VIMS' best views of Sinlap Crater, and as such were used by Le Mouélic et al. (2008) to map that crater.

3.4. Shikoku flybys (T8, T10, T12, T14)

Interspersed with the Fensal–Aztlan passes described above were passes with subspacecraft longitudes between 146°W and 161°W that show the distinctive Shikoku Facula ("Great Britain") prominently, including T8, T10, T12, and T14 (though Ta, Tb, and T3 might fit in this category as well). Barnes et al. (2007) used the coarse-resolution, but long integration time and uniform coverage of the T8 data for global mapping.

The T10 data have a good moderate-resolution sequence of the area from Adiri to Tui Regio viewed from gibbous phase. Ádámkovics et al. (2008) used this viewing geometry to constrain Xanadu's surface scattering phase function. The T12 dataset shows Xanadu and its environs in a gibbous phase at moderate resolution, while T14 has only coarse global coverage. T8, T10, and T12 were used by Nelson et al. (2006) to monitor Hotei Regio.

3.5. Southward bound sequence (T16–T24)

From T16 onward, Titan was illuminated on egress rather than on ingress. The T16–T24 sequence has *Cassini*'s subspacecraft point over the dayside progress southward from 8°S to 55°S, and eastward from 17°E to 50°E. The latter portion of the sequence, particularly T20 through T24, represent VIMS' best views that it will ever get of the south pole given the onset of southern winter. Most of this sequence shows clouds either at the south pole or near 40°S latitude (Rodriguez, 2008).

On T16 the VIMS team first tested the "noodle" technique for data acquisition that is described by Barnes et al. (2008). In the T16 case, during a slow CIRS scan from Titan's north pole to the south pole, VIMS repeatedly acquired 64×1 strips that we merged together for the projection shown in Fig. 3.

T17 has a moderate-resolution mosaic of mid-southern latitudes near the sub-Saturn longitude, and T18 is a mix of resolutions that includes a fine-resolution 1×3 mosaic near the evening terminator. We only have coarse, global-level data from T19.

The T20 flyby was an important one for VIMS. Using noodle mode, VIMS acquired repeated N-by-1 lines, letting the relative motion between Titan and the spacecraft trace out the second spatial dimension. The inbound noodle passed over northwestern Fensal, and acquired data with spatial sampling approaching 500 m/pixel. The inbound noodle passed over a candidate cryovolcanic vent that had been previously identified by RADAR (Lopes et al., 2007). LeCorre et al. (2008) analyzed the spectral character of possible outflows, comparing them in particular to that of Tortola Facula. Barnes et al. (2008) identified sand-free interdunes of varying composition between individual sand dunes, and mapped the orientation and separation of the dunes seen in the T20 inbound noodle. Jaumann et al. (2008) studied the erosional and depositional processes ongoing in Pacman Bay off of south Quivira, using it as an analog for the *Huygens* landing site. Finally, this flyby also contains high quality moderate-resolution cubes of the south pole proper.

T21 and T23 are both coarse-resolution flybys, but both managed to capture morphologically and positionally distinct cloud formations (Rodriguez, 2008). The ingress views from these flybys, obtained from over Titan's nightside with phase angle over 90°, are shown in Fig. 7. Similarly interesting clouds are present in the T22 and T24 flyby datasets (Rodriguez, 2008). T22 also has a moderate-resolution mosaic of extremeo southwestern Senkyo and the curvilinear bright/dark markings south of there, while T24 offers another moderate-resolution view of Titan's south pole.

3.6. North polar sequence (T25–T33)

The T25–T33 flyby sequence starts with the egress, dayside asymptote starting over mid-northern latitudes and changing uniformly equatorward over the course of the sequence. The subspacecraft point varies relatively smoothly from 51°N 121°E to 0°N 142°E. These flybys show small clouds extended along lines of latitude within 30° of the north pole that Brown et al. (2008) interpret as lake-effect clouds. These are most prominent in the T26–T29, and T33 cloud-color images in Figs. 4 and 5. T26 and T27 have corresponding crescent views in Fig. 7, where T27 shows a spectacular cloud deck near the south pole.

The data for T25 are few and of coarse spatial resolution because most of the data from this flyby did not make it down to the ground. VIMS got a single ISS-ridealong global mosaic at ~25 km/pixel on egress, and nothing more. These data did, however, present our earliest view of the north polar lakes and seas, and as such were used by Brown et al. (2008) to compare VIMS observations of Kraken Mare to the view from RADAR. T26, T27, T29, and T30 have global-level views from a mid-northerly perspective.

The T28, T31, and T32 have some of our best moderate-resolution views of Titan's mid-northern latitudes due to their low emission angle and more northerly subsolar point. These cubes revealed a set of parallel, linear dark markings oriented roughly radial to Titan's anti-Saturn point; we label them as "T28 Virgae" in Fig. 1. T33 is VIMS' first recognizable view of Selk Crater, identified by Soderblom (2008) based on its morphological similarity to Sinlap Crater.

3.7. T34

T34 is a unique flyby. It was acquired while using Titan to steer *Cassini* to targeted flybys of Saturn's other icy satellites, and as such does not fall into one of the longer sequences. It offers a

singular viewing geometry, representing the only opportunity that VIMS has had to view territory in the longitude range 20°E through 90°E. This area encompasses the Senkyo dunefields and their environs. Barnes et al. (2008) included a fine-resolution view of these dunefields, but its resolution was insufficient to unambiguously detect the dunes directly. The VIMS team continues to work on this valuable dataset.

3.8. Adiri sequence (T35–T44)

The latter Titan flybys from *Cassini*'s prime mission have been used in fewer published papers to this point because the VIMS team has had less time to analyze them. Several studies of these data are presently ongoing or nearing completion, including Rodriguez (2008) who used these sequences up to T38 to complete their global view of Titan's cloud distribution since SOI. The sequence from T35 through the end of the prime mission after T44 all have good views of the bright area named Adiri, which is located just west of the Huygens landing site.

T35 has moderate-resolution views of Adiri, Selk Crater, and western Shangri-La obtained from nearly directly above the Huygens landing site. The views on T36, T39, T41, and T43 were restricted to long-distance, global observations. We show a view of the T43 ingress showing equatorial clouds in Fig. 7 (see also Griffith et al., 2008). The T37 flyby has global views with a single noodle, a cube obtained near enough to closest approach that apparent surface motion extends the cube's geometrical projection out in the direction of flight. The noodle starts near the western edge of Shikoku and covers a sliver of eastern Senkyo and Mindanao Facula (''Ireland'').

VIMS observed at closest approach on the T38 flyby in order to obtain fine-resolution imaging spectroscopy of the enigmatic southern Ontario Lacus. Using this dataset Brown et al. (2008) identified an absorption due to liquid ethane within Ontario Lacus, confirming it to indeed be a lake of liquid hydrocarbon. Barnes (2009) studied the lake's morphology, finding evidence for past lake-level changes based on concentric rings of distinct spectral character surrounding the lake. Both of the aforementioned authors used the four data cubes that show the lake to infer atmospheric properties from the emission phase function. On egress after closest approach, VIMS obtained moderate-resolution views of both Selk Crater and strange dark linear markings within Dilmun.

T40 has fine-resolution observations of Selk crater that were analyzed by Soderblom (2008), and moderate-resolution views of the Huygens landing site and an unnamed set of Virgae NNW of Selk. The red spot in the T40 view shown in Fig. 5 is an uncorrected cosmic-ray hit in the 5-μm band. The T42 flyby also has a good view of the unnamed Virgae and the region to their west. The best moderate-resolution cubes from T44 were on ingress, and that view is the one that we show in Fig. 6. They show the area from eastern Tui Regio to Hotei Regio and northward, viewed at moderately high phase angle.

4. Future observations

Further exploration of Titan will take place during the *Cassini* Equinox mission. This extended mission began at the end of the prime mission, 2008 July 1, and will last for two years, ending 2010 June 30. It contains 26 additional close Titan flybys, numbered T45 through T70. VIMS is planned to acquire global-scale views on each of the flybys, and will obtain fine-resolution observations of the Huygens landing site on T47 in addition to other data that we will detail after the completion of the *Cassini* Equinox misson.

Acknowledgements

JWB acknowledges the support of the *Cassini* VIMS team. The authors acknowledge the support of the *Cassini* project from both NASA and ESA. Thanks to Alfred McEwen and Robert West for constructive reviews.

References

Acton, C.H., 1999. SPICE products available to the planetary science community. In: Lunar and Planetary Institute Conference Abstracts, pp. 1233–1234.

Ádámkovics, M., de Pater, I., Hartung, M., Barnes, J.W., 2008. Evidence for condensed-phase methane enhancement over Xanadu on Titan. Planet. Space Sci., this issue.

Adriani, A., Moriconi, M.L., Liberti, G.L., Gardini, A., Orosei, R., D'Aversa, E., Filacchione, G., Coradini, A., 2005. Titan's ground reflectance retrieval from Cassini–VIMS data taken during the July 2ND, 2004 fly-by at 2 AM UT. Earth Moon and Planets 96, 109–117.

Baines, K.H., Drossart, P., Lopez-Valverde, M.A., Atreya, S.K., Sotin, C., Momary, T.W., Brown, R.H., Buratti, B.J., Clark, R.N., Nicholson, P.D., 2006. On the discovery of CO nighttime emissions on Titan by Cassini/VIMS: derived stratospheric abundances and geological implications. Planetary and Space Science 54, 1552–1562.

Baines, K.H., Drossart, P., Momary, T.W., Formisano, V., Griffith, C., Bellucci, G., Bibring, J.P., Brown, R.H., Buratti, B.J., Capaccioni, F., Cerroni, P., Clark, R.N., Coradini, A., Combes, M., Cruikshank, D.P., Jaumann, R., Langevin, Y., Matson, D.L., McCord, T.B., Mennella, V., Nelson, R.M., Nicholson, P.D., Sicardy, B., Sotin, C., 2005. The atmospheres of Saturn and Titan in the near-infrared first results of Cassini/VIMS. Earth Moon and Planets 96, 119–147.

Barnes, J.W., 2009. Shoreline features of Titan's Ontario Lacus from Cassini/VIMS observations. Icarus 201 (1), 217–225.

Barnes, J.W., Brown, R.H., Radebaugh, J., Buratti, B.J., Sotin, C., Le Mouelic, S., Rodriguez, S., Turtle, E.P., Perry, J., Clark, R., Baines, K.H., Nicholson, P.D., 2006. Cassini observations of flow-like features in western Tui Regio, Titan. Geophysical Research Letters 33, 16204.

Barnes, J.W., Brown, R.H., Soderblom, L., Buratti, B.J., Sotin, C., Rodriguez, S., Le Mouèlic, S., Baines, K.H., Clark, R., Nicholson, P., 2007. Global-scale surface spectral variations on Titan seen from Cassini/VIMS. Icarus 186, 242–258.

Barnes, J.W., Brown, R.H., Soderblom, L., Sotin, C., Le Mouèlic, S., Rodriguez, S., Jaumann, R., Beyer, R.A., Buratti, B.J., Pitman, K., Baines, K.H., Clark, R., Nicholson, P., 2008. Spectroscopy, morphometry, and photoclinometry of Titan's dunefields from Cassini/VIMS. Icarus 195, 400–414.

Barnes, J.W., Brown, R.H., Turtle, E.P., McEwen, A.S., Lorenz, R.D., Janssen, M., Schaller, E.L., Brown, M.E., Buratti, B.J., Sotin, C., Griffith, C., Clark, R., Perry, J., Fussner, S., Barbara, J., West, R., Elachi, C., Bouchez, A.H., Roe, H.G., Baines, K.H., Bellucci, G., Bibring, J.-P., Capaccioni, F., Cerroni, P., Combes, M., Coradini, A., Cruikshank, D.P., Drossart, P., Formisano, V., Jaumann, R., Langevin, Y., Matson, D.L., McCord, T.B., Nicholson, P.D., Sicardy, B., 2005. A 5-μm-bright spot on Titan: evidence for surface diversity. Science 310, 92–95.

Barnes, J.W., Radebaugh, J., Brown, R.H., Wall, S., Soderblom, L., Lunine, J., Burr, D., Sotin, C., Le Mouélic, S., Rodriguez, S., Buratti, B.J., Clark, R., Baines, K.H., Jaumann, R., Nicholson, P.D., Kirk, R.L., Lopes, R., Lorenz, R.D., Mitchell, K., Wood, C.A., 2007. Near-infrared spectral mapping of Titan's mountains and channels. Journal of Geophysical Research (Planets) 112.

Brown, M.E., Schaller, E.L., Roe, H.G., Chen, C., Roberts, J., Brown, R.H., Baines, K.H., Clark, R.N., 2008. Discovery of lake-effect clouds on Titan. ArXiv e-prints.

Brown, R.H., Baines, K.H., Bellucci, G., Bibring, J.-P., Buratti, B.J., Capaccioni, F., Cerroni, P., Clark, R.N., Coradini, A., Cruikshank, D.P., Drossart, P., Formisano, V., Jaumann, R., Langevin, Y., Matson, D.L., McCord, T.B., Mennella, V., Miller, E., Nelson, R.M., Nicholson, P.D., Sicardy, B., Sotin, C., 2004. The Cassini visual and infrared mapping spectrometer (VIMS) Investigation. Space Science Reviews 115, 111–168.

Brown, R.H., Baines, K.H., Bellucci, G., Buratti, B.J., Capaccioni, F., Cerroni, P., Clark, R.N., Coradini, A., Cruikshank, D.P., Drossart, P., Formisano, V., Jaumann, R., Langevin, Y., Matson, D.L., McCord, T.B., Mennella, V., Nelson, R.M., Nicholson, P.D., Sicardy, B., Sotin, C., Baugh, N., Griffith, C.A., Hansen, G.B., Hibbitts, C.A., Momary, T.W., Showalter, M.R., 2006. Observations in the Saturn system during approach and orbital insertion, with Cassini's visual and infrared mapping spectrometer (VIMS). A&A 446, 707–716.

Brown, R.H., Soderblom, L.A., Soderblom, J.M., Clark, R.N., Jaumann, R., Barnes, J.W., Sotin, C., Buratti, B., Baines, K.H., Nicholson, P.D., 2008. The identification of liquid ethane in Titan's Ontario Lacus. Nature 454, 607–610.

Buratti, B.J., Sotin, C., Brown, R.H., Hicks, M.D., Clark, R.N., Mosher, J.A., McCord, T.B., Jaumann, R., Baines, K.H., Nicholson, P.D., Momary, T., Simonelli, D.P., Sicardy, B., 2006. Titan: preliminary results on surface properties and photometry from VIMS observations of the early flybys. Planetary and Space Science 54, 1498–1509.

Clark, R., Curchin, J.M., Brown, R.H., Cruikshank, D.P., Jaumann, R., Lunine, J., Hoefen, T.H., Baines, K.H., Buratti, B.J., Barnes, J.W., Nicholson, P., Stephan, K., 2007. Detection of widespread aromatic and aliphatic hydrocarbon deposits on Titan, submitted for publication.

Griffith, C.A., Penteado, P., Baines, K., Drossart, P., Barnes, J., Bellucci, G., Bibring, J., Brown, R., Buratti, B., Capaccioni, F., Cerroni, P., Clark, R., Combes, M., Coradini, A., Cruikshank, D., Formisano, V., Jaumann, R., Langevin, Y., Matson, D., McCord, T., Mennella, V., Nelson, R., Nicholson, P., Sicardy, B., Sotin, C., Soderblom, L.A., Kursinski, R., 2005. The evolution of Titan's mid-latitude clouds. Science 310, 474–477.

Griffith, C.A., Penteado, P., Rannou, P., Brown, R., Boudon, V., Baines, K.H., Clark, R., Drossart, P., Buratti, B., Nicholson, P., McKay, C.P., Coustenis, A., Negrao, A., Jaumann, R., 2006. Evidence for a polar ethane cloud on Titan. Science 313, 1620–1622.

Griffith, C.A., McKay, C.P., Ferri, G., 2008. Titan's Tropical Storms in an evolving atmosphere. The Astrophysical Journal 687 (1), L41–L44.

Jaumann, R., Brown, R.H., Stephan, K., Barnes, J.W., Soderblom, L.A., Sotin, C., Le Mouélic, S., Clark, R.N., Soderblom, J., Buratti, B.J., Wagner, R., McCord, T.B., Rodriguez, S., Baines, K.H., Cruikshank, D.P., Nicholson, P.D., Griffith, C.A., Langhans, M., Lorenz, R.D., 2008. Fluvial erosion and post-erosional processes on Titan. Icarus 197, 526–538.

Jaumann, R., Stephan, K., Brown, R.H., McCord, T.B., Coradini, A., Capaccioni, F., Filacchione, G., Clark, R.N., Cerroni, P., Baines, K.H., Belluchi, G., Bibring, J.-P., Buratti, B.J., Bussoletti, E., Combes, M., Cruikshank, D.P., Drossart, P., Formisano, V., Langevin, Y., Matson, D.L., Nelson, R.M., Nicholson, P.D., Sicardy, B., Sotin, C., Roatsch, T., Scholten, F., Matz, K.-D., 2006. High resolution Cassini–VIMS mosaics of Titan and the icy Saturnian satellites. Planetary and Space Science 54 (12), 1146–1155.

Le Mouélic, S., Paillou, P., Janssen, M.A., Barnes, J.W., Rodriguez, S., Sotin, C., Brown, R.H., Baines, K.H., Buratti, B.J., Clark, R.N., Crapeau, M., Encrenaz, P.J., Jaumann, R., Geudtner, D., Paganelli, F., Soderblom, L., Tobie, G., Wall, S., 2008. Mapping and interpretation of Sinlap crater on Titan using Cassini VIMS and RADAR data. Journal of Geophysical Research (Planets) 113, 4003.

LeCorre, L., Le Mouélic, S., Sotin, C., Barnes, J.W., Brown, R.H., Buratti, B., Jaumann, R., Rodriguez, S., Soderblom, L.A., Clark, R., Baines, K., Nicholson, P., 2008. Analysis of a cryolava flow on Titan with VIMS infrared images. Planetry and Space Science 57 (7), doi:10.1016/j.pss.2009.03.005.

Lopes, R.M.C., Mitchell, K.L., Stofan, E.R., Lunine, J.I., Lorenz, R., Paganelli, F., Kirk, R.L., Wood, C.A., Wall, S.D., Robshaw, L.E., Fortes, A.D., Neish, C.D., Radebaugh, J., Reffet, E., Ostro, S.J., Elachi, C., Allison, M.D., Anderson, Y., Boehmer, R., Boubin, G., Callahan, P., Encrenaz, P., Flamini, E., Francescetti, G., Gim, Y., Hamilton, G., Hensley, S., Janssen, M.A., Johnson, W.T.K., Kelleher, K., Muhleman, D.O., Ori, G., Orosei, R., Picardi, G., Posa, F., Roth, L.E., Seu, R., Shaffer, S., Soderblom, L.A., Stiles, B., Vetrella, S., West, R.D., Wye, L., Zebker, H.A., 2007. Cryovolcanic features on Titan's surface as revealed by the Cassini Titan radar mapper. Icarus 186, 395–412.

Lorenz, R.D., Wall, S., Radebaugh, J., Boubin, G., Reffet, E., Janssen, M., Stofan, E., Lopes, R., Kirk, R., Elachi, C., Lunine, J., Mitchell, K., Paganelli, F., Soderblom, L., Wood, C., Wye, L., Zebker, H., Anderson, Y., Ostro, S., Allison, M., Boehmer, R., Callahan, P., Encrenaz, P., Ori, G.G., Francescetti, G., Gim, Y., Hamilton, G., Hensley, S., Johnson, W., Kelleher, K., Muhleman, D., Picardi, G., Posa, F., Roth, L., Seu, R., Shaffer, S., Stiles, B., Vetrella, S., Flamini, E., West, R., 2006. The sand seas of Titan: Cassini RADAR observations of longitudinal dunes. Science 312, 724–727.

McCord, T.B., Hansen, G.B., Buratti, B.J., Clark, R.N., Cruikshank, D.P., D'Aversa, E., Griffith, C.A., Baines, E.K.H., Brown, R.H., Dalle Ore, C.M., Filacchione, G., Formisano, V., Hibbitts, C.A., Jaumann, R., Lunine, J.I., Nelson, R.M., Sotin, C., 2006. Composition of Titan's surface from Cassini VIMS. Planetary and Space Science 54, 1524–1539 (The Cassini VIMS Team).

McCord, T.B., Hayne, P., Combe, J.-P., Hansen, G.B., Barnes, J.W., Rodriguez, S., Le Mouélic, S., Baines, E.K.H., Buratti, B.J., Sotin, C., Nicholson, P., Jaumann, R., Nelson, R., 2008a. Titan's surface: search for spectral diversity and composition using the Cassini VIMS investigation. Icarus 194, 212–242 (The Cassini Vims Team).

McCord, T.B., Hayne, P., Combe, J.-P., Hansen, G.B., Barnes, J.W., Rodriguez, S., Le Mouèlic, 2008b. Titan's surface: search for spectral diversity and composition using the Cassini VIMS investigation. Icarus 194 (1), 212–242.

Nelson, R.M., Brown, R.H., Hapke, B.W., Smythe, W.D., Kamp, L., Boryta, M.D., Leader, F., Baines, K.H., Bellucci, G., Bibring, J.-P., Buratti, B.J., Capaccioni, F., Cerroni, P., Clark, R.N., Combes, M., Coradini, A., Cruikshank, D.P., Drossart, P., Formisano, V., Jaumann, R., Langevin, Y., Matson, D.L., McCord, T.B., Mennella, V., Nicholson, P.D., Sicardy, B., Sotin, C., 2006. Photometric properties of Titan's surface from Cassini VIMS: relevance to Titan's hemispherical albedo dichotomy and surface stability. Planetary and Space Science 54, 1540–1551.

Nelson, R.M., Kamp, L.W., Matson, D.L., Irwin, P.G.J., Baines, K.H., Boryta, M.D., Leader, F.E., Jaumann, R., Smythe, W.D., Sotin, C., Clark, R.N., Cruikshank, D.P., Drossart, P., Pearl, J.C., Hapke, B.W., Lunine, J., Combes, M., Bellucci, G., Bibring, J.-P., Capaccioni, F., Cerroni, P., Coradini, A., Formisano, V., Filacchione, G., Langevin, R.Y., McCord, T.B., Mannella, V., Nicholson, P.D., Sicardy, B., 2009. Saturn's Titan: surface change, ammonia, and implications for atmospheric and tectonic activity. Icarus, accepted for publication.

Rodriguez, S., 2008. Titan cloud distributions from Cassini VIMS, Nature, in press.

Rodriguez, S., Le Mouélic, S., Sotin, C., Clénet, H., Clark, R.N., Buratti, B., Brown, R.H., McCord, T.B., Nicholson, P.D., Baines, K.H., 2006. Cassini/VIMS hyperspectral observations of the HUYGENS landing site on Titan. Planetary and Space Science 54, 1510–1523 (The VIMS Science Team).

Soderblom, J.M., 2008. Selk crater. Planetary and Space Science, this issue.

Soderblom, L., Kirk, R.L., Lunine, J.I., Anderson, J.A., Baines, K.H., Barnes, J.W., Barrett, J.M., Brown, R.H., Buratti, B.J., Clark, R.N., Cruikshank, D.P., Elachi, C., Janssen, M.A., Jaumann, R., Karkoschka, E., Le Mouèlic, S., Lopes, R.M., Lorenz, R.D., McCord, T.B., Nicholson, P.D., Radebaugh, J., Rizk, B., Sotin, C., Stofan, E.R., Sulcharski, T.L., Tomasko, M.G., Wall, S.D., 2007. Correlations between Cassini VIMS spectra and RADAR SAR images: implications for Titan's surface composition and the character of the Huygens probe landing site. Planetary and Space Science, in press, doi:10.1016/j.pss.2007.04.014.

Sotin, C., Jaumann, R., Buratti, B.J., Brown, R.H., Clark, R.N., Soderblom, L.A., Baines, K.H., Bellucci, G., Bibring, J.-P., Capaccioni, F., Cerroni, P., Combes, M., Coradini, A., Cruikshank, D.P., Drossart, P., Formisano, V., Langevin, Y., Matson, D.L., McCord, T.B., Nelson, R.M., Nicholson, P.D., Sicardy, B., Le Mouèlic, S., Rodriguez, S., Stephan, K., Scholz, C.K., 2005. Release of volatiles from a possible cryovolcano from near-infrared imaging of Titan. Nature 435, 786–789.